Inorganic Chemistry

Communication

pubs.acs.org/IC

$Th(H_2O)(I^VO_3)_2[I^{VII}_{0.6}V_{1.76}O_7(OH)]$: A Mixed-Valent Iodine Compound Containing Periodate Stabilized by Crystallographically Compatible Lattice Sites

Yaxing Wang,[†,‡] Linjuan Zhang,[§] Lanhua Chen,[†,‡] Weifeng Li,[†,‡] Xing Dai,[†,‡] Juan Diwu,[†,‡] Jianqiang Wang,[§] Zhifang Chai,[†,‡] and Shuao Wang*[,†,‡]

[†]School for Radiological and Interdisciplinary Sciences (RAD-X), Soochow University, 199 Renai Road, Suzhou Industrial Park, China

[‡]Collaborative Innovation Center of Radiation Medicine of Jiangsu Higher Education Institutions, 199 Renai Road, Suzhou Industrial Park, China

[§]Shanghai Institute of Applied Physics, Chinese Academy of Sciences, 2019 JiaLuo Road, Shanghai 201800, China

Supporting Information

ABSTRACT: Periodate is a strong oxidant and is often reduced to IO_3^- or I_2 under hydrothermal conditions. Here, we present a rare case of a mixed-valent iodate(V)/periodate(VII) compound, $Th(H_2O)(I^VO_3)_2[I^{VII}_{0.6}V_{1.76}O_7(OH)]$, prepared with a hydrothermal method starting from periodic acid. Crystallographic results demonstrate that heptavalent iodine adopts $I^{VII}O_6$ distorted octahedral geometries, which are stabilized on the crystallographically compatible crystal lattice sites of VO_6 octahedra through an aliovalent substitutional disorder mechanism. X-ray photoelectron and synchrotron radiation X-ray absorption spectroscopes both quantitatively confirm the presence of mixed valent iodine oxoanions with a molar ratio (I^V/I^{VII}) of 4:1, consistent with the single crystal X-ray analysis. The crystallization of mixed-valent products with compatible lattice site can be fancily utilized for stabilizing the uncommon oxidation states of other elements in general.

The actinide oxoanion compounds, such as actinide-based iodate, silicate, phosphate, and borate, have been extensively investigated in the past two decades.[1] These compounds not only offer chances to investigate divergence or parallel chemistry between 4f and 5f elements but also provide molecular level insights into the environmental fate and nuclear waste forms of actinides.[2] Particularly, actinide iodates have received remarkable attention due to the application of iodate as a precipitation reagent for separation purposes in the fuel cycle, as well as their implications on the fate of ^{129}I, which is one of the long-lived radionuclides ($t_{1/2}$ = 1.5 × 10^7 y) with major concerns.[3] Iodine often exists in three common oxidation states: −1, 0, and +5, where the latter is present as the trigonal pyramid IO_3^- anion under the oxidative environment.[4a] An extremely rare case of tetraoxoiodate IO_4^{3-} was reported in $Ag_4(UO_2)_4(IO_3)_2(IO_4)_2O_2$ as a new type of pentavalent iodine-based oxoanion.[5] By contrast, heptavalent iodine is much less explored given its strong oxidative power ($E°(IO_4^-/IO_3^-)$ = 1.6 V).[4] It is often found in a six-coordinated periodate anion IO_6^{5-} and is easily reduced to IO_3^- or I_2 under a variety of conditions.[4] As one of a limited number of examples, IO_6^{5-} was found in $K_2[(UO_2)_2(VO)_2(IO_6)_2O]\cdot H_2O$ due to the presence of high valent vanadium to preserve an oxidative condition during the hydrothermal reaction.[6] In fact, the only example of mixed-valent I(V/VII) reported in the literature, I_2O_6, which was initially thought to be the hexavalent iodine oxide, contains separated lattice sites for both IO_3^- and IO_6^{5-} units confirmed by its single crystal structure.[7] This unique compound was isolated more than 20 years ago through controlled dehydration of H_5IO_6 by Kraft et al., and there is no other mixed-valent iodine compound reported. Nevertheless, materials and compounds constructed from mixed-valent oxoanions are of particular importance, not only because of the aesthetics of structural design but also because of the development of potential applications in magnetism, conductivity, and optical properties.[8−11]

During our continuous efforts in understanding the structure−property relationship of actinide oxoanion compounds, the second mixed-valent iodate(V)/periodate(VII) compound $Th(H_2O)(I^VO_3)_2[I^{VII}_{0.6}V_{1.76}O_7(OH)]$ (**ThIVO**) was discovered, which can be isolated from the hydrothermal reaction of $Th(NO_3)_4\cdot 6H_2O$ and V_2O_5 with a large excess of H_5IO_6. Although IO_6^{5-} is significantly reduced to IO_3^- during the reaction, heptavalent iodine partially incorporates onto VO_6 sites in an aliovalent substitutional disorder mechanism, providing a new strategy to stabilize this uncommon oxidation state of iodine. This compound is stable exposed to air for at least three months.

As shown in Figure 1a, the crystal structure of **ThIVO** is a complex dense 3D framework crystallizing in the triclinic space group $P\bar{1}$. The structure can be divided into three fragments: ThO_9 polyhedra, IO_3 trigonal pyramids, and complex $[I^{VII}_{0.6}V_{1.76}O_7(OH)]^{2-}$ chains. The Th center is bound by nine oxygen atoms, which are provided by IO_3, VO_6, VO_4, and a coordinated water molecule, forming a tricapped trigonal prism. The Th−O bond lengths are within a range from 2.386(6) Å to 2.583(6) Å, which is normal. The I−O bond lengths in the IO_3

Received: August 18, 2016
Published: November 17, 2016

DOI: 10.1021/acs.inorgchem.6b02010
Inorg. Chem. 2016, 55, 12101−12104

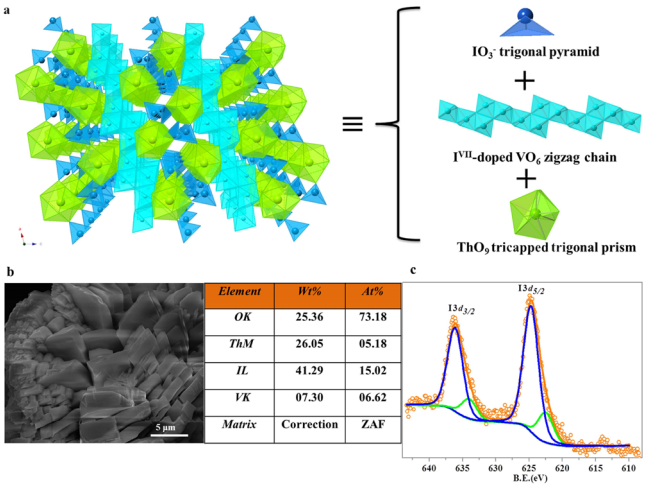

Figure 1. (a) Structural view of dense 3D frameworks along the *b* axis. The IO_3 trigonal pyramid is shown in blue. The ThO_9 polyhedra are shown in green, and the I^{VII}-doped VO_6 zigzag chain is shown in cyan. (b) SEM image of the ThIVO clusters. Elemental analysis indicates that the Th/I/V ratio is similar to the ratio determined by crystallography. (c) I3d XPS spectrum. Green and blue lines correspond to I^{VII} and I^{V}, respectively. The yellow line is the fitted spectrum, which is in agreement with the experimental result.

trigonal pyramids are also typical, ranging from 1.793(5) Å to 1.814(6) Å. $[I^{VII}_{0.6}V_{1.76}O_7(OH)]^{2-}$ consists of an I^{VII}-doped VO_6 zigzag chain (Figure 1a), distorted $I(5)^{VII}O_6$, and distorted $V(3)O_4$, with the last two sites showing relatively low occupancies of 0.15 and 0.21, respectively. I^{VII}-doped VO_6 zigzag chains are constructed of dimers of edge-sharing $V(1)O_6$ that are perpendicular to the dimers of the edge-sharing $V(2)O_6$ polyhedra. Two different coordination geometries of the VO_6 polyhedral are observed in the zigzag chains: [1 + 4 + 1] coordination of the $V(1)O_6$ polyhedra with one vanadyl bond length of 1.775(9) Å (O(10)) and the [2 + 2 + 2] coordination of the $V(2)O_6$ polyhedra with two vanadyl bond lengths of 1.703(6) Å (O(5)) and 1.766(6) Å (O(9)) (as illustrated in Figure S2).[12] A relatively short distance between adjacent oxygen atoms is observed in $[I^{VII}_{0.6}V_{1.76}O_7(OH)]^{2-}$. In addition, the results from bond valence sum (BVS) calculations (Tables S1 and S2) suggest that terminal oxygen atom O(5) is protonated to be a hydroxyl unit.[13] The O−O distances are in the range from 2.7 to 3.2 Å, forming a hydrogen-bond network.

Notably, the isotropic atomic displacement parameter (U_{eq}) were unreasonably small (as shown in Figure S1a) when the V was only assigned to VO_6 sites, leading to the initial speculation of I incorporation on these sites. However, unreasonably large U_{eq} values were obtained when I was solely assigned to the VO_6 sites compared to those when I was assigned to IO_3 sites (0.050 $Å^2$ and 0.077 $Å^2$ vs 0.007 $Å^2$ and 0.009 $Å^2$, as shown in Figure S1b), indicating the presence of aliovalent substitutional disorder between I^{VII} and V^{V} at these sites. Therefore, a standard substitutional disorder treatment (detailed refinement processes are included in the cif file) was used to refine the precise site occupancy factors (SOFs) of V and I. The refinement results demonstrate that the occupancy factors of I for the two sites are 0.33 and 0.12, respectively, providing a total I^{VII}/V^{V} crystallographic ratio in these sites of 0.45:1.55. In addition, the substitutional disorder is also present in the structure solution of the lower symmetry space group *P*1. Using the bond distances within the XO_6 units, the bond valence sums of iodine calculated using the I−O parameter are 6.8 and 6.4, respectively. This slight divergence from 7 is a result of substitutional disorder, where the bond distances of V−O play a role.

Energy-dispersive spectroscopy (EDS) analysis indicates that the I/Th/V atomic ratio in the bulk sample is 15.02:5.18:6.62%, which is highly consistent with the atomic ratio in the formula for **ThIVO** determined by X-ray crystallography (Figure 1b). Moreover, ICP-OES measurement on dissolved crystals afforded an I/Th/V molar ratio of 8.57:3.67:4.38, also close to the theoretical value of 2.6:1:1.76. Thermalgravimetric/differential scanning calorimetry (TG/DSC) analysis was also performed on dried samples from 30 to 900 °C. As shown in Figure S3, the weight loss of 3% below 350 °C should be attributed with the loss of coordinated water and hydroxyl groups. As shown in Figures S4 and S5, the infrared vibrational frequencies of I−O and V−O are superimposed below 1000 cm^{-1}; however, a feature at 937 cm^{-1} in the Raman spectrum is clearly indicative of vanadyl in **ThIVO**.[6] In addition, the IR spectrum exhibits the characteristic vibrations of OH^- and H_2O at 3400−3500 cm^{-1} ν(O−H) and 1600 cm^{-1} δ(H−O−H), respectively. The Raman spectrum recorded on **ThIVO** also contains features for ν(O−H) located above 3000 cm^{-1}.

X-ray photoelectron spectroscopy (XPS) was further utilized to determine the oxidation state of iodine in **ThIVO**, as shown in Figure 1c. The well-resolved peaks correspond to the binding energies (BEs) of $3d_{3/2}$ and $3d_{2/5}$ of iodine (V and VII), which are consistent with the previously reported values.[14] The peaks at 624.7 and 636.1 eV are assigned to the BE of I^{V}, and the two resolved shoulders at 622.5 and 634 eV confirm the presence of I^{VII}. The quantitative peak area ratio of I^{V}/I^{VII} obtained from the fitting results (Figure S6 and Table S3) is 4.18, which is in good agreement with the crystallographic results.

To further investigate the valence state of iodine, we collected X-ray absorption spectroscopy (XAS) data to directly clarify the structural divergence of the various oxidation states of iodine. Figure 2a shows the iodine *K*-edge XAS spectrum of **ThIVO**,

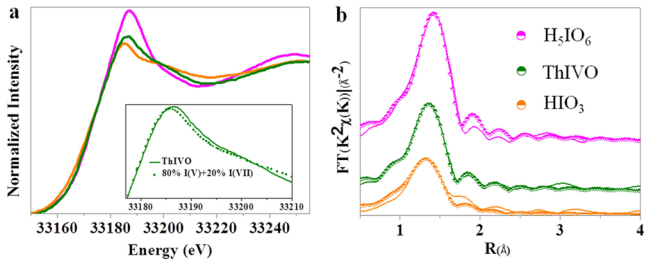

Figure 2. (a) XANES spectra of synthesized compounds (**ThIVO**, olive line) and reference iodine species (H_5IO_6 magenta line, HIO_3 orange line). Inset: The fitted ratio of I^{V}/I^{VII} obtained from the XANES data was approximately equal to 80:20% in **ThIVO**. (b) Extended X-ray absorption fine structure (EXAFS) fitting (scatter line) and experimental spectra (solid line) of synthesized compounds (**ThIVO**) and reference iodine species.

along with those for H_5IO_6 and HIO_3, which serve as the reference materials for I^{VII} and I^{V}, respectively. The white line in the iodine *K*-edge XAS spectrum corresponds to the electronic transitions from 1s to 5p states. As a result, the intensity of this feature reflects the unoccupied states. The I^{V} ion spectrum contains a relatively weak main peak and a shoulder at the higher energy region (approximately 15 eV); this shoulder is strongly correlated with the bond length of I−O because of the scattering contribution. In the cases of I^{VI} and I^{VII}, the intensity of the main

DOI: 10.1021/acs.inorgchem.6b02010
Inorg. Chem. 2016, 55, 12101−12104

peak gradually increases and the position shifts to higher energy with the increase of oxidation states. For the **ThIVO** sample, the intensity and energy position of the main peaks are similar but still deviate from that of I^{V}, implying the presence of mixed oxidation states (corresponding to different iodine occupied sites). According to the crystallographic and XPS analysis, the I^{V}/I^{VII} ratio is approximately 4:1. Therefore, we carried out a simple simulation by superimposing the I^{V} and I^{VII} spectra using the proposed molar ratio of I^{V}/I^{VII} and comparing the result with the spectra of the **ThIVO** samples, as shown in the inset of Figure 2a. The almost overlap in the intensity and position of the main peak between the experimental data and simulation results again quantitatively confirms the presence of I^{V} and I^{VII} and corresponding aliovalent substitutional disorder.

Quantitative information was also extracted using extended X-ray absorption fine structure (EXAFS) fitting, as shown in Figures 2b and S7 and in Table 1. Pentavalent iodine exhibits

Table 1. Bond Parameters of I−O Obtained from EXAFS Experimental Data

	coordination number	bond length/Å	bond disorder $\sigma^2 \times 10^{-3}/Å^2$	R factor
HIO_3	3.1 ± 0.2	1.81 ± 0.02	5.1 ± 0.8	0.008
H_5IO_6	6.0 ± 0.2	1.87 ± 0.02	2.4 ± 0.7	
ThIVO	3.6 ± 0.2	1.82 ± 0.02	1.9 ± 0.8	

coordination number of 3 with a relatively short I−O bond length of 1.81 Å. However, six-coordinated oxygen atoms were resolved in the spectrum of the H_5IO_6 reference sample, with the longest I−O bond length being 1.87 Å. In particular, mixed-valent iodine is clearly present in the **ThIVO** sample, which corresponds to a mediate coordination number and I−O bond length provided by EXAFS in conjunction with the crystallographic results. Notably, the averaged coordination number of the **ThIVO** determined by EXAFS is 3.6, which is also in high agreement with the calculated averaged coordination number assuming a I^{V}/I^{VII} molar ratio of 4:1.

In conclusion, a rare case of mixed-valent iodate(V)/periodate(VII) compound $Th(H_2O)(I^{V}O_3)_2[I^{VII}_{0.6}V_{1.76}O_7(OH)]$ is successfully isolated and structurally characterized. A detailed structural analysis combined with spectroscopic techniques including XPS, XANES, and EXAFS clearly reveals that a robust inorganic lattice in conjunction with compatible crystal lattice sites can trap thermodynamically unstable oxoanions, providing a new synthetic strategy to stabilize the uncommon oxidation states of other elements in general.

■ ASSOCIATED CONTENT

Supporting Information

The Supporting Information is available free of charge on the ACS Publications website at DOI: 10.1021/acs.inorgchem.6b02010.

X-ray crystallographic files (CIF)

Detailed experimental methods, X-ray diffraction patterns, infrared and Raman spectra, XPS, UV−vis spectroscopy, and TG/DSC (PDF)

■ AUTHOR INFORMATION

Corresponding Author

*E-mail: shuaowang@suda.edu.cn.

ORCID

Shuao Wang: 0000-0002-1526-1102

Notes

The authors declare no competing financial interest.

■ ACKNOWLEDGMENTS

This work was supported by grants from the National Science Foundation of China (91326112, 21422704, U1532259), the Science Foundation of Jiangsu Province (BK20140007), a Project Funded by the Priority Academic Program Development of Jiangsu Higher Education Institutions (PAPD) and Jiangsu Provincial Key Laboratory of Radiation Medicine and Protection, and "Young Thousand Talented Program" in China.

■ REFERENCES

(1) (a) Baker, R. J. Oxoanion systems containing trivalent actinides. *Coord. Chem. Rev.* **2014**, *266−267*, 123−136. (b) Polinski, M. J.; Villa, E. M.; Albrecht-Schmitt, T. E. Oxoanion systems containing trivalent actinides. *Coord. Chem. Rev.* **2014**, *266−267*, 16−27. (c) Burns, P. C. U^{6+} minerals and inorganic compounds: Insights into an expanded structural hierarchy of crystal structures. *Can. Mineral.* **2005**, *43*, 1839−1894. (d) Lee, C.-S.; Wang, S.-L.; Lii, K.-H. $Cs_2K(UO)_2Si_4O_{12}$: A Mixed-valence uranium(IV,V) silicate. *J. Am. Chem. Soc.* **2009**, *131*, 15116−15117. (e) Morrison, G.; Smith, M. D.; zur Loye, H.-C. Understanding the formation of salt-inclusion phases: an enhanced flux growth method for the targeted synthesis of salt-inclusion cesium halide uranyl silicates. *J. Am. Chem. Soc.* **2016**, *138*, 7121−7129. (f) Abraham, F.; Arab-Chapelet, B.; Rivenet, M.; Tamain, C.; Grandjean, S. Actinide oxalates, solid state structures and applications. *Coord. Chem. Rev.* **2014**, *266−267*, 28−68. (g) Yang, W.; Parker, T. G.; Sun, Z. Structural chemistry of uranium phosphonates. *Coord. Chem. Rev.* **2015**, *303*, 86−109. (h) Andrews, M. B.; Cahill, C. L. Uranyl bearing hybrid materials: synthesis, speciation, and solid-state structures. *Chem. Rev.* **2013**, *113*, 1121−1136.

(2) (a) Burns, P. C.; Ikeda, Y.; Czerwinski, K. Advances in actinide solid-state and coordination chemistry. *MRS Bull.* **2010**, *35*, 868−876. (b) Ewing, R. C.; Runde, W.; Albrecht-Schmitt, T. E. Environmental impact of the nuclear fuel cycle: fate of actinides. *MRS Bull.* **2010**, *35*, 859−866. (c) Knope, K. E.; Soderholm, L. Solution and solid-state structural chemistry of actinide hydrates and their hydrolysis and condensation products. *Chem. Rev.* **2013**, *113*, 944−994. (d) Silver, M. A.; Albrecht-Schmitt, T. E. Evaluation of f-element borate chemistry. *Coord. Chem. Rev.* **2016**, *323*, 36−51.

(3) (a) Aldahan, A.; Alfimov, V.; Possnert, G. ^{129}I anthropogenic budget: major sources and sinks. *Appl. Geochem.* **2007**, *22*, 606−618. (b) Hou, X.; Povinec, P. P.; Zhang, L.; Shi, K.; Biddulph, D.; Chang, C.-C.; Fan, Y.; Golser, R.; Hou, Y.; Jeskovsky, M.; Jull, A. J. T.; Liu, Q.; Luo, M.; Steier, P.; Zhou, W. Iodine-129 in seawater offshore fukushima: distribution, inorganic speciation, sources, and budget. *Environ. Sci. Technol.* **2013**, *47*, 3091−3098.

(4) (a) Runde, W.; Bean, A. C.; Albrecht-Schmitt, T. E.; Scott, B. L. Structural characterization of the first hydrothermally synthesized plutonium compound, $PuO_2(IO_3)_2{\cdot}H_2O$. *Chem. Commun.* **2003**, *4*, 478−479. (b) Sykora, R. E.; Ok, K. M.; Halasyamani, P. S.; Albrecht-Schmitt, T. E. Structural modulation of molybdenyl iodate architectures by alkali metal cations in $AMoO_3(IO_3)$ (A = K, Rb, Cs): a facile route to new polar materials with large SHG responses. *J. Am. Chem. Soc.* **2002**, *124*, 1951−1957. (c) Yang, B. P.; Hu, C. L.; Xu, X.; Mao, J. G. New series of polar and nonpolar platinum iodates $A_2Pt(IO_3)_6$ (A = H_3O, Na, K, Rb, Cs). *Inorg. Chem.* **2016**, *55*, 2481−2487.

(5) Bean, A. C.; Campana, C. F.; Kwon, O.; Albrecht-Schmitt, T. E. A new oxoanion: $[IO_4]^{3-}$ containing I(V) with a stereochemically active lone-pair in the silver uranyl iodate tetraoxoiodate(V), $Ag_4(UO_2)_4(IO_3)_2(IO_4)_2O_2$. *J. Am. Chem. Soc.* **2001**, *123*, 8806−8810.

(6) Sykora, R. E.; Albrecht-Schmitt, T. E. Self-assembly of a polar open-framework uranyl vanadyl hexaoxoiodate(VII) constructed entirely from distorted octahedral building units in the first uranium

DOI: 10.1021/acs.inorgchem.6b02010
Inorg. Chem. 2016, 55, 12101−12104

hexaoxoiodate:$K_2[(UO_2)_2(VO)_2(IO_6)_2O]\cdot H_2O$. *Inorg. Chem.* **2003**, *42*, 2179−2181.
(7) Kraft, T.; Jansen, M. Synthesis and crystal structure of diiodine(V/VII) hexaoxide: an intermediate between a molecular and a polymer solid. *J. Am. Chem. Soc.* **1995**, *117*, 6795−6796.
(8) Yu, N.; Klepov, V. V.; Kegler, P.; Bosbach, D.; Albrecht-Schmitt, T. E.; Alekseev, E. V. $Th(As^{III}_4As^{V}_4O_{18})$: a mixed-valent oxoarsenic(III)/arsenic(V) actinide compound obtained under extreme conditions. *Inorg. Chem.* **2014**, *53*, 8194−8196.
(9) Villa, E. M.; Alekseev, E. V.; Depmeier, W.; Albrecht-Schmitt, T. E. Syntheses, structures, and comparisons of thallium uranium phosphites, mixed phosphate-phosphites, and phosphate. *Cryst. Growth Des.* **2013**, *13*, 1721−1729.
(10) Gui, D.; Zheng, T.; Chen, L.; Wang, Y.; Li, Y.; Sheng, D.; Diwu, J.; Chai, Z.; Albrecht-Schmitt, T. E.; Wang, S. Hydrolytically stable nanoporous thorium mixed phosphite and pyrophosphate framework generated from redox-active ionothermal reactions. *Inorg. Chem.* **2016**, *55*, 3721−3123.
(11) (a) Wu, Q.; Li, Y.-G.; Wang, Y.-H.; Wang, E.-B.; Zhang, Z.-M.; Clérac, R. Mixed-valent $\{Mn_{14}\}$ aggregate encapsulated by the inorganic polyoxometalate shell: $[Mn^{III}_{13}Mn^{II}O_{12}(PO_4)_4(PW_9O_{34})_4]^{31-}$. *Inorg. Chem.* **2009**, *48*, 1606−1612. (b) Haider, A.; Ibrahim, M.; Bassil, B. S.; Carey, A. M.; Viet, A. N.; Xing, X.; Ayass, W. W.; Miñambres, J. F.; Liu, R.; Zhang, G.; Keita, B.; Mereacre, V.; Powell, A. K.; Balinski, K.; N'Diaye, A. T.; Küpper, K.; Chen, H.-Y.; Stimming, U.; Kortz, U. mixed-valent Mn_{16}-containing heteropolyanions: tuning of oxidation state and associated physicochemical properties. *Inorg. Chem.* **2016**, *55*, 2755−2764. (c) Lin, J.; Diefenbach, K.; Fu, J.; Cross, J. N.; Clark, R. J.; Albrecht-Schmitt, T. E. $LnV_3Te_3O_{15}(OH)_3\cdot nH_2O$ (Ln = Ce, Pr, Nd, Sm, Eu, Gd; n = 1−2): a new series of semiconductors with mixed-valent tellurium (IV,VI) oxoanions. *Inorg. Chem.* **2014**, *53*, 9058−9064. (d) Sturza, M.; Bugaris, D. E.; Malliakas, C. D.; Han, F.; Chung, D. Y.; Kanatzidis, M. G. Mixed-valent $NaCu_4Se_3$: a two-dimensional metal. *Inorg. Chem.* **2016**, *55*, 4884−4890. (e) Daub, M.; Scherer, H.; Hillebrecht, H. Synthesis, crystal structure, and spectroscopy of the mixed-valent boroseleniteselenate $B_2Se_3O_{10}$. *Inorg. Chem.* **2015**, *54*, 2325−2330. (f) Song, S. Y.; Lee, D. W.; Ok, K. M. Rich structural chemistry in scandium selenium/tellurium oxides: mixed-valent selenite−selenates, $Sc_2(SeO_3)_2(SeO_4)$ and $Sc_2(TeO_3)(SeO_3)(SeO_4)$, and ternary tellurite, $Sc_2(TeO_3)_3$. *Inorg. Chem.* **2014**, *53*, 7040−7046.
(12) Schindler, M.; Hawthorne, F. C.; Baur, W. H. Crystal chemical aspects of vanadium: polyhedral geometries, characteristic bond valences, and polymerization of (VO_n) polyhedral. *Chem. Mater.* **2000**, *12*, 1248−1259.
(13) Brese, N. E.; O'Keeffe, M. Bond-valence parameters for solids. *Acta Crystallogr., Sect. B: Struct. Sci.* **1991**, *47*, 192−197.
(14) (a) Sherwood, P. M. A. X-ray photoelectron spectroscopic studies of some iodine compounds. *J. Chem. Soc., Faraday Trans. 2* **1976**, *72*, 1805−1820. (b) Mansour, A. N.; Melendres, C. A. Characterization of $KNiIO_6$ by XPS. *Surf. Sci. Spectra* **1994**, *3*, 287−295.

DOI: 10.1021/acs.inorgchem.6b02010
Inorg. Chem. 2016, 55, 12101−12104